

a computational point of view, although the 6-31G* basis is necessary to reproduce the overall activation energy, the 2-in-2/631G results are virtually the same as 6-in-6/6-31G* in describing relative energy changes in the vicinity of the saddle point, where overlap between the termini is small.

Acknowledgment. We are deeply indebted to Dr. Paul Saxe

of Los Alamos National Laboratory for helpful comments and to the National Science Foundation for Grant CHE84-21140. M.P. acknowledges support from the Office of Naval Research through the Naval Research Laboratory.

Registry No. Trimethylene biradical, 32458-33-6; cyclopropane, 75-19-4.

Unimolecular Thermal Reaction of Formaldoxime at High Temperatures: Experiments and Calculations

Ko Saito,* Koso Makishita, Terumitsu Kakumoto, Takaharu Sasaki, and Akira Imamura

Department of Chemistry, Faculty of Science, Hiroshima University, Higashisenda, Naka-ku, Hiroshima 730, Japan (Received: October 19, 1987; In Final Form: February 9, 1988)

The thermal decomposition of formaldoxime diluted in Ar has been studied behind reflected shock waves over the temperature range between 1050 and 1300 K and the total density range of $(0.6\text{--}2.4) \times 10^{-5}$ mol cm⁻³. The decomposition process was monitored using the vacuum-UV absorption of the reactant and the IR emission from HCN. It was found that the main thermal reaction proceeded via (1) $\text{H}_2\text{CNOH} \rightarrow \text{H}_2\text{O} + \text{HCN}$ and that the alternate isomerization (2) $\text{H}_2\text{CNOH} \rightarrow \text{CH}_3\text{NO}$ was negligible. Over the temperature range of the study, the decomposition rate constant is $k_1 = 10^{12.65} \exp(-48 \text{ kcal mol}^{-1}/RT)$ s⁻¹. There is a very slight pressure dependence over the experimental region. Ab initio MO calculations were performed for the decomposition and the isomerization channels. The barrier height for the isomerization was higher than that for the molecular decomposition by 24 kcal mol⁻¹ at the MP2/3-21G level. Rate constants calculated for the dehydration step were in good agreement with those measured.

Introduction

Formaldoxime ($\Delta H_f^\circ = 0$ kcal/mol) is an isomer of formamide ($\Delta H_f^\circ = -44.5$ kcal/mol) and nitrosomethane ($\Delta H_f^\circ = 16$ kcal/mol). At high temperatures formamide decomposes to ammonia and carbon monoxide but it does not isomerize to its isomers since these processes require complicated bond rearrangements.¹ The thermal isomerization of nitrosomethane to formaldoxime was investigated by Batt and Gowenlock² by a flow method at 4.5 Torr over a temperature range of 633–698 K. They reported a rate constant, $k_{-2} = 10^{8.9} \exp(-29.1 \text{ kcal mol}^{-1}/RT)$ s⁻¹, for this isomerization. Later Benson and O'Neal estimated a value, $k_{-2} = 10^{12.9} \exp(-39.3 \text{ kcal mol}^{-1}/RT)$ s⁻¹, on the basis of assumed parameters for the transition state of this reaction.³ Taylor and Bender⁴ studied thermal decomposition of formaldoxime using a static method over the temperature range of 623–688 K and at 4.5 Torr. They found that the reaction produced mainly water and hydrogen cyanide with a rate constant $k_1 = 10^{9.5} \exp(-39 \text{ kcal mol}^{-1}/RT)$ s⁻¹. On the basis of the abnormally low preexponential factor, Benson and O'Neal² suggested that the experiments were affected by oxygen and wall effects. Thus, we have no reliable kinetic data for these elementary reactions in a homogeneous system. For the determination of an elementary reaction rate constants, it is necessary to avoid several problems arising from secondary and heterogeneous reactions. In the current states, we determine the rate constant for the primary thermal reaction of formaldoxime in Ar at high temperatures behind shock waves where complications of the type mentioned above are avoided. In addition, we have calculated transition-state structures for plausible reaction paths by means of a molecular orbital method. The results are compared with those from the experiments.

Experimental Section

The experimental measurements were conducted behind reflected shock waves at temperatures between 1050 and 1300 K and in the density range $(0.6\text{--}2.4) \times 10^{-5}$ mol cm⁻³ using mixtures containing 0.1, 0.5, and 1.0 mol % formaldoxime diluted in Ar. Formaldoxime trimer was prepared by the reaction of a formaldehyde solution and hydroxylamine as described in ref 5. The product was tested by CHN elemental analysis. The monomer was generated by heating the trimer to about 135 °C and then diluted with Ar to about 1% in a 6-L glass flask. The decrease of the monomer concentration in the flask was checked several times according to a spectroscopic method. The results indicated that the polymerization was negligible over a period of a few days.

The shock-tube equipment used in this work was the same as that used in a previous study.⁶ The test section was about 3.8 m long with a 9.4-cm i.d. It was evacuated to less than 2×10^{-6} Torr before each run. A pair of MgF₂ windows was mounted on the tube walls 2 cm upstream from the end plate. Time-resolved optical measurements of the reaction were performed through these windows.

Several chemical species were monitored during the course of the reaction by their IR emission, UV absorption, and vacuum-UV absorption. In the IR region, several fundamental bands of HCN (ν_1 and ν_3) and H₂O (ν_1 and ν_3) were selected by means of interference filters with an average half-bandwidth of $\Delta\lambda = 0.2 \mu\text{m}$. The IR emission intensity was detected by an AuGe element cooled at 77 K. The time constant of the detection system was determined to be about 15 μs by using the CO₂ fundamental bands.

Measurements of UV and vacuum-UV absorptions were performed at the same position as the IR observation. The wavelengths observed were 121.6, 130.5, 216, and 308 nm for the detection of H, O, CH₃, and OH, respectively. A microwave discharge tube containing flowing He with a few percent of ad-

(1) Kakumoto, T.; Saito, K.; Imamura, A. *J. Phys. Chem.* **1985**, *89*, 2286.

(2) Batt, L.; Gowenlock, B. G. *Trans. Faraday Soc.* **1960**, *56*, 182.

(3) Benson, S. W.; O'Neal, H. E. *Kinetic Data on Gas Phase Unimolecular Reactions*; NSRDS-NBS 21; U.S. Government Printing Office: Washington, DC, 1970.

(4) Taylor, H. A.; Bender, H. *J. Chem. Phys.* **1941**, *9*, 761.

(5) Scoll, R. *Chem. Ber.* **1891**, *24*, 573.

(6) Saito, K.; Kakumoto, T.; Imamura, A. *J. Phys. Chem.* **1984**, *88*, 1182.

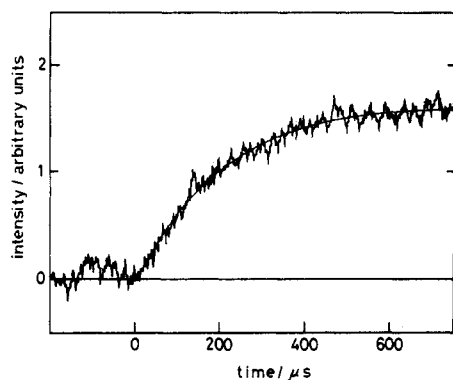


Figure 1. Typical IR emission profile at 3.0 μm ($\text{HCN } \nu_3$). Conditions: temperature = 1265 K; total density = $1.1 \times 10^{-5} \text{ mol cm}^{-3}$; 0.5 mol % CH_2NOH in Ar.

ditions was used as a radiation light source. For the purpose of qualitative analysis of the shock-heated gas component, the gas was removed from the shock tube and was analyzed by GC and IR.

Results and Discussion

The IR emission due to HCN fundamental bands showed a growth with time as shown in Figure 1 for the $\text{HCN } \nu_3$ band. All emission traces were expressed simply as $I = I_\infty(1 - e^{-kt})$, where I_∞ corresponds to a steady intensity after the long reaction time and k is the first-order rate constant for the HCN production. Similar traces were obtained for the $\text{HCN } \nu_1$ band. At higher temperatures I_∞ values were obtained directly from each trace, but at lower temperatures the intensity did not reach its steady level within the reaction time. In such cases, I_∞ was evaluated from an extrapolation of high-temperature values with the temperature dependence corresponding to the observing wavelength. Thus, the first-order rate constant for the HCN production was obtained from each emission trace. Figure 2 shows an Arrhenius plot of k . Over the total density range, which covers a factor of 4 in magnitude, the rate constant seems almost constant within experimental errors although the data at the highest density are slightly larger. An Arrhenius plot fit to a straight line which is expressed as

$$k = 10^{12.65} \exp(-48 \text{ kcal mol}^{-1}/RT) \text{ s}^{-1}$$

Since there is significant scatter in the data, these Arrhenius parameters include large uncertainties. We estimate the error in k is about a factor of 2. The uncertainty with regard to the activation energy is $\pm 2.5 \text{ kcal mol}^{-1}$, in the experimental temperature range studied.

The emission at 2.7 μm showed the contributions from the reactant (OH stretching) and H_2O (ν_1 and ν_3). A quantitative analysis of the emission intensity at the later stage of the reaction time, where the reactant decomposed mostly, showed that the amount of the water produced was nearly the same as the initial concentration of the reactant. From this result and the fact that there is no change in the rate constant by changing the reactant concentration over a factor of 10, the main route of the decomposition is thought to be the molecular fission



The preexponential factor, $10^{12.65}$, is not unreasonable for reaction 1 having a tight transition state. Also, considering the very slight pressure effect on the rate constant, the reaction is thought to be near the high-pressure region.

The absorption in the UV region was observed at 216 nm for CH_3 radical and at 308 nm for OH radical. The absorption coefficient of CH_3 at 216 nm has been reported to be $1.8 \times 10^6 \text{ cm}^2 \text{ mol}^{-1}$ around 1400 K with fwhm = 1.6 nm.⁷ This was applied to the present investigation for the quantitative analysis of the

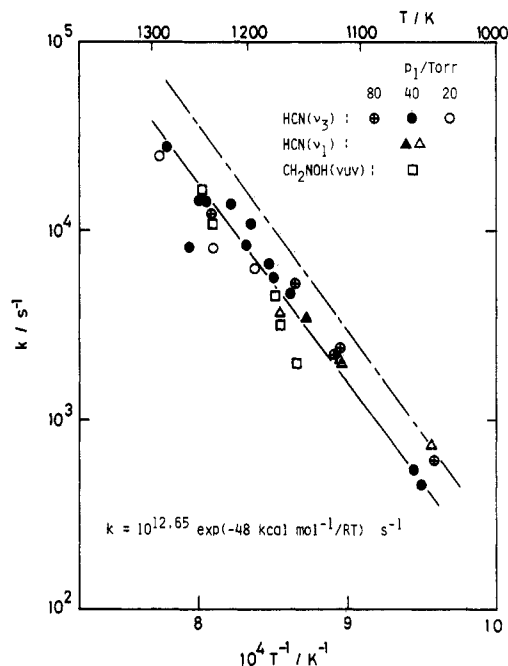


Figure 2. Arrhenius plot of first-order rate constants obtained from production of HCN and from decay of reactant. A broken line corresponds to the theoretical calculation for reaction 1.

absorption data. For a reactant concentration of $1.2 \times 10^{-7} \text{ mol cm}^{-3}$, no absorption was observed at this wavelength within the reaction time, meaning that CH_3 was less than a few percent of the reactant. Also, we did not observe any absorption at 308 nm. By use of the calibration curve for the OH absorption at 308 nm,⁸ this experimental fact means that the concentration of OH produced in the present system is found to be less than $6 \times 10^{-10} \text{ mol cm}^{-3}$ or 0.5% of the reactant. From these observations it appears that the following reactions are negligibly small under the present conditions



since nitrosomethane is thought to decompose easily to CH_3 and NO under the present experimental conditions. Another reaction route which produces H-atom was checked by observing the H-atom absorption at 121.6 nm (Lyman α). At this wavelength there was no absorption by H-atom but there was a strong absorption by the reactant. That is, the absorption rose sharply at incident and reflected shock fronts and then decayed exponentially with time. A typical absorption trace is shown in Figure 3. Alternate observations were performed at 130.5 nm by using an O-atom resonance lamp for the comparison with the absorption at 121.6 nm. The absorption profile was the same as Figure 3, meaning that no detectable H-atoms were produced under the present conditions. Therefore, reactions which produce H-atom such as reaction 5 are unimportant under the present conditions.



From the absorption traces at 121.6 and 130.5 nm, rate constants for the reactant decay were obtained at an early stage of the reaction. These are also plotted in Figure 2, giving the same results with the rate constants for the HCN production.

A theoretical prediction of the rate constant for the unimolecular reaction may be obtained by using transition-state theory. That is, we can estimate high-pressure rate constants for the possible reaction paths on the basis of the entropy of activation and the heat of activation. These thermochemical parameters are eval-

(7) Zabel, F. *Int. J. Chem. Kinet.* 1977, 9, 651.

(8) Saito, K.; Ito, R.; Kakumoto, T.; Imamura, A. *J. Phys. Chem.* 1986, 90, 1422.

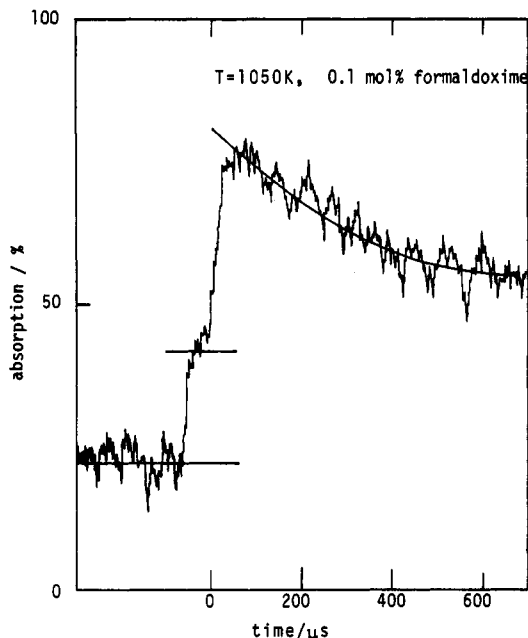


Figure 3. Typical vacuum-UV absorption trace at 121.6 nm. Conditions: temperature = 1050 K; total density = 1.0×10^{-5} mol cm^{-3} ; 0.1 mol % CH_2NOH in Ar.

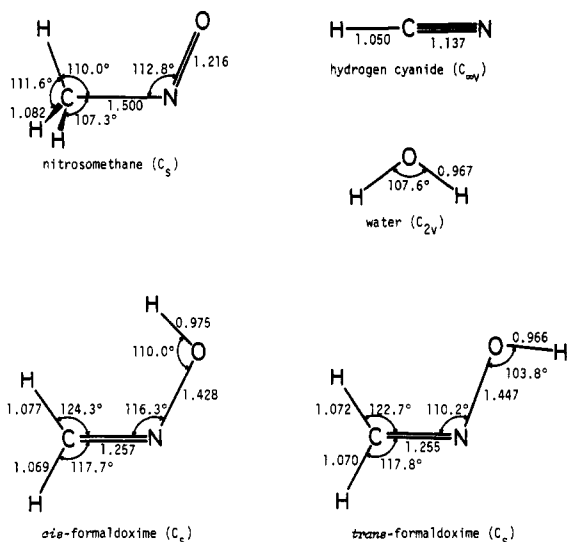


Figure 4. HF/3-21G optimized geometries for hydrogen cyanide, water, nitrosomethane, and *trans*- and *cis*-formaldoxime. Bond distances are in angstroms and angles are in degrees.

uated in terms of structures, total energies, and vibrational frequencies for the reactant and the transition state corresponding to each reaction path. Here, we report molecular orbital calculations for reactions 1 and 2. The calculations were performed for formaldoxime, nitrosomethane, hydrogen cyanide, and water and for two transition states corresponding to reactions 1 and 2. We used the closed-shell Hartree-Fock method using the 3-21G basis set for the geometry optimizations. The vibrational analysis were done at the 3-21G level by the analytical differentiation of the energy gradient. For the present purpose the geometries and the vibrational frequencies calculated at this level seem to be sufficient to discuss the reaction mechanism. However, since calculated energies at the same level may be insufficient for the quantitative discussion, we applied Møller-Plesset second-order perturbation method (MP2) at the HF/3-21G optimized geometries. The programs used were GAUSSIAN 80,⁹ GAUSSIAN 82,¹⁰ and

(9) Binkley, J. S.; Whiteside, R. A.; Krishnam, R.; Seeger, R.; DeFrees, D. J.; Schlegel, H. B.; Topil, S.; Kahn, L. R.; Pople, J. A. *QCPE* 1980, 102, 939; Program Library of Institute for Molecular Science.

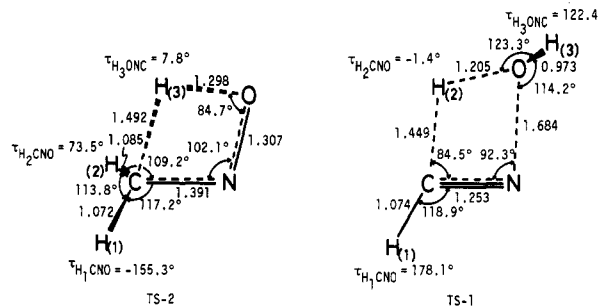


Figure 5. HF/3-21G optimized geometries of transition states for the decomposition of formaldoxime. Bond distances are in angstroms and angles are in degrees. τ , dihedral angle, is defined as positive clockwise.

TABLE I: Relative Energies and Heats of Formation (in kcal mol^{-1})

	CH_3NO	TS-2	<i>cis</i> - CH_2NOH	<i>trans</i> - CH_2NOH	TS-1	HCN + H_2O
HF/3-21G	22.0	101.0	8.6	0.0	68.4	-26.7
MP2/3-21G ^a	14.5	78.7	6.6	0.0	58.2	
$\Delta H_f^\circ_{300}$	16 ^b			0 ^c		-25.5 ^b

^a At HF/3-21G optimized geometries. ^b Benson, S. W. *Thermochemical Kinetics*, 2nd ed; Wiley: New York, 1976. ^c Reference 3.

TABLE II: Experimental and Calculated Vibrational Frequencies of *trans*-Formaldoxime

sym species	no.	mode	frequency/ cm^{-1}		
			ν_{exptl}	ν_{calcd}	$\nu_{\text{calcd}}/\nu_{\text{exptl}}$
A'	1	OH stretch	3646	3883.7	1.065
	2	CH_2 stretch	3098	3416.6	1.103
	3	CH_2 stretch	2976	3316.1	1.114
	4	CN stretch	1642	1869.5	1.139
	5	CH_2 bend	1410	1596.8	1.132
	6	NOH bend	1315	1449.2	1.102
	7	CH_2 rock	1154	1298.7	1.125
	8	NO stretch	888	993.9	1.119
	9	CNO bend	535	546.0	1.021
A''	10	CH_2 wag	949	1172.1	1.235
	11	CH_2 twist	770	868.2	1.128
	12	CN-OH twist	420	366.5	0.873

GAMES.¹¹

Good agreement was obtained for the structural parameters between the observed and calculated values for the stable molecules. That is, the differences are within 2.7% in bond distance and 1.9% in bond angle. Figure 4 shows calculated geometries for the stationary structures. Figure 5 shows optimized geometries for TS-1 for reaction 1 and TS-2 for reaction 2. It appears that, in TS-1, the H(3) atom which is connected to the oxygen atom is significantly out of the CNO plane and the H(2) atom is only very slightly out of this plane. As is discussed later, the TS-1 reaction coordinate is clearly that with the imaginary frequency and is the motion corresponding to the reaction producing H_2O and HCN. In the case of TS-2, which is also a four-center, the H(3) atom in the four-membered ring is out of the CNO plane. It is found that, as reaction proceeds along the reaction path, the angle $\angle\text{NOH}(3)$ decreases and the OH(3) bond distance increases. Considering the results of the vibrational analysis, it appears that the H(3) atom migrates to the carbon atom to produce a methyl radical.

Table I lists calculated relative energies for the molecules and TS's. It is seen that the relative energies decrease particularly in the TS's when the MP2 method is used. The difference of the total energies between the two paths is about 24 kcal mol^{-1} . In the lowest line in Table I, experimental heats of formation are

(10) Binkley, J. S.; Frish, M. J.; DeFrees, D. J.; Raghavachari, K.; Whiteside, R. A.; Schlegel, H. B.; Fluder, E. M.; Pople, J. A. GAUSSIAN82; Carnegie-Mellon University: Pittsburgh, PA, 1985; Program Library of Institute for Molecular Science.

(11) Dupuis, M.; Sprangler, D.; Wedolski, J. J. GAMES; QG01; Program Library of Institute for Molecular Science.

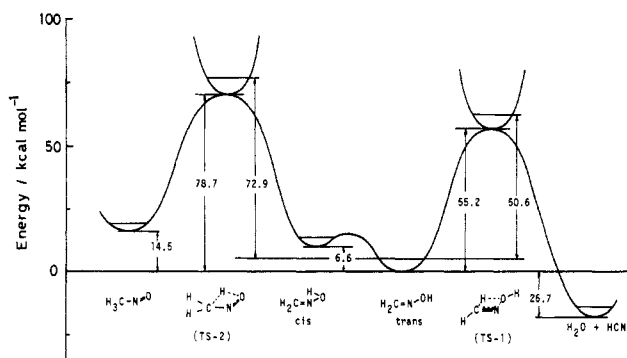
TABLE III: HF/3-21G Calculated Vibrational Frequencies (in cm^{-1}) for Two Transition States

	TS-1	TS-2
	511.3	693.6
	546.0	868.9
	895.8	937.6
	988.8	1128.6
	1047.4	1222.8
	1170.1	1248.0
	1459.1	1361.4
	1663.1	1637.0
	2106.2	2108.5
	3351.2	3213.8
	3807.3	3394.5
	2023.8i	2702.4i

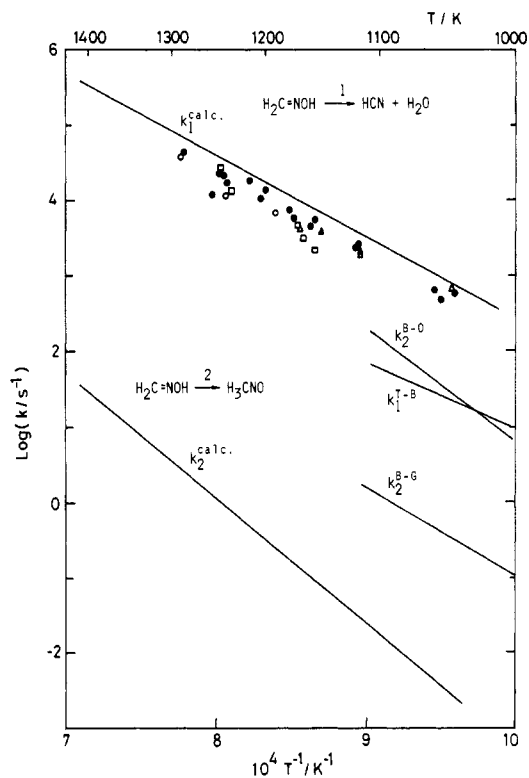
TABLE IV: Evaluations of Preexponential Factors^a

T/K	σ^1/σ	I^1/I	$Q_{\text{vib}}^1/Q_{\text{vib}}$	$\log(A/\text{s}^{-1})$
Reaction 1				
1400	1/1	1.330	0.776 (0.765)	13.42 (13.41)
1500			0.767 (0.755)	13.44 (13.44)
Reaction 2				
1400	1/1	0.984	0.385 (0.369)	13.05 (13.03)
1500			0.373 (0.359)	13.06 (13.05)

^aValues in parentheses were calculated by using 10% scaled frequencies. σ is the symmetry number, I the moment of inertia, and Q_{vib} the vibrational partition function.

**Figure 6.** Relative energies for the decomposition of formaldoxime by MP2/3-21G calculations.

shown for the stable molecules which are consistent with the calculated values using the MP2 method. Table II lists the calculated and the experimental vibrational frequencies for *trans*-formaldehyde. The experimental values are cited from ref 12. The last column shows the ratio $\nu_{\text{calcd}}/\nu_{\text{exptl}}$, indicating that the harmonic frequencies calculated are systematically overestimated by about 10% relative to the experimental anharmonic frequencies as was also seen in other cases.¹³ Table III shows the results of the vibrational analysis for TS-1 and TS-2. With the calculated values in Tables II and III the preexponential factors of the rate constants were evaluated for the two channels at various temperatures. In Table IV, the results are listed for 1400 and 1500 K. The A factor for reaction 1 is larger than that for reaction 2 by about a factor of 2. Figure 6 shows a potential energy diagram for this reaction system. The potential barriers are shown with and without zero-point energy corrections. From the large difference between TS-1 and TS-2, 24 kcal mol^{-1} , it is predicted

**Figure 7.** Comparison of the rate constants concerning reactions 1 and 2. Experimental results are shown by the same symbols shown in Figure 2. B-G, B-O, and T-B are the results cited from ref 2, 3, and 4, respectively.

that reaction 1 proceeds more easily than reaction 2, which is consistent with the experimental results.

Results of the ab initio calculations for k_1 are compared with the experimental results in Figure 7 (and in Figure 3). It appears that the theoretical calculations of k_1 give satisfactory agreement with the experimental measurements. Considering that in the present MO calculations we did not use more sophisticated basis sets, it is surprising that the calculated threshold energy (50.6 kcal mol^{-1}) agrees with the experimental activation energy within a few kcal mol^{-1} . Previous experimental data obtained at lower temperatures²⁻⁴ are shown as extrapolated lines in Figure 7. For reaction 1, there are strong discrepancies between the extrapolation for the previous data for $k_1(\text{T-B})$,⁴ obtained at temperatures lower than 700 K, and the present experimental and theoretical results. As stated in the Introduction, the experiment of Taylor and Bender⁴ was possibly affected by oxygen and wall effects. This seems to cause a much lower temperature dependence of the rate constant ($E_a = 39 \text{ kcal mol}^{-1}$). The shock-tube technique has the advantage of avoiding heterogeneous catalytic and secondary bimolecular reactions which take place in static and flow systems. For reaction 2, $k_2(\text{B-G})$ and $k_2(\text{B-O})$ values which were estimated from the reported k_{-2} values and the heat of reaction are much higher than the calculated value. In the present study, we could not determine k_2 values experimentally because of its very small branching ratio compared to that of reaction 1. According to the calculations, the ratio k_1/k_2 is about 5×10^4 at 1200 K. This fact supports the experimental result that the products from reaction 2 were not observed during the reaction. For the comparison between experiments and calculations, it is necessary to measure directly the rate of reaction 2.

Registry No. Formaldoxime, 75-17-2.

(12) Califano, S.; Luttke, W. *Z. Phys. Chem. (Munich)* **1956**, *6*, 83.

(13) Kakumoto, T.; Saito, K.; Imamura, A. *J. Phys. Chem.* **1987**, *91*, 2366.